Spatiotemporal Airy Light Bullets in the Linear and Nonlinear Regimes

Daryoush Abdollahpour,[1,2,*] Sergiy Suntsov,[1] Dimitrios G. Papazoglou,[1,3] and Stelios Tzortzakis[1,†]

[1]*Institute of Electronic Structure and Laser, Foundation for Research and Technology Hellas, P.O. Box 1527, 71110, Heraklion, Greece*
[2]*Physics Department, University of Crete, 71003, Heraklion, Greece*
[3]*Materials Science and Technology Department, University of Crete, P.O. Box 2208, 71003, Heraklion, Greece*

We demonstrate the realization of intense Airy-Airy-Airy (Airy³) light bullets by combining a spatial Airy beam with an Airy pulse in time. The Airy³ light bullets belong to a family of linear spatiotemporal wave packets that do not require any specific tuning of the material optical properties for their formation and withstand both diffraction and dispersion during their propagation. We show that the Airy³ light bullets are robust up to the high intensity regime, since they are capable of healing the nonlinearly induced distortions of their spatiotemporal profile.

One of the major challenges in optics is the generation of localized optical wave packets. As proposed by Silberberg [1], such localized waves, called light bullets due to their particlelike nature, are feasible in the context of nonlinear optics where the Kerr nonlinearity may compensate the effect of diffraction and dispersion. The generation of stable nonlinear 3D (localized in both space and time) light bullets is a very delicate task [2], since it is possible only when the effects of dispersion and diffraction are equalized [1,2]. Furthermore, these light bullets are very sensitive to any modulation or structural instability [3]. On the other hand, in the linear propagation regime, several nondiffracting, nondispersing wave packets have been demonstrated with the Bessel beam being perhaps the most studied case in the spatial domain [4], while in the spatiotemporal domain the linear light bullets were either *X* waves [5] or *O* waves [6] for normal and anomalous dispersions, respectively. Recently, a new kind of nonspreading optical waves, the Airy beams, has been demonstrated by Siviloglou *et al.* [7,8]. Airy beams in the extreme nonlinear optics regime were implemented for the first time in Ref. [9], while spatiotemporal oblique Airy wave packets have been discussed in Ref. [10]. Airy functions are unique since they are the only dispersion-free solution in one dimension [7,11]. This effectively enables the disentanglement of space and time in the 3D spatiotemporal propagation problem. Following the theoretical prediction of Siviloglou *et al.* [7], Chong *et al.* [12] have demonstrated the generation of versatile linear light bullets consisting of a Bessel distribution in space and an Airy temporal profile. Since the space-time decoupling in the linear propagation regime is possible, a wave packet comprised of an Airy pulse and a nondiffracting beam such as Bessel, Airy, or Mathieu beams [13] will propagate as a light bullet without the need for equalization of diffraction and dispersion. Such versatile linear 3D light bullets open up new exciting possibilities in numerous applications. However, for high intensity applications such as filamentation [14], electric discharge triggering and guiding [15], and remote sensing [16,17], a question that arises is how the bullet will be affected when its peak intensity is high enough to cause strong nonlinearities. In contrast to the Gaussian wave packets, these linear light bullets rely on a strong energy redistribution mechanism induced by their specific spatiotemporal profile that redirects energy from a low intensity reservoir to the high intensity peak. This makes the propagation of such wave packets in the high intensity regime quite interesting, since the linear redistribution mechanism competes in the spatiotemporal domain with nonlinear effects such as the optical Kerr effect, multiphoton or tunnel ionization, and nonlinear losses [14].

In this Letter, we report on the experimental demonstration of Airy³ light bullets. These light bullets are described by an Airy distribution in all spatial and temporal dimensions. Moreover, we show that, going from the linear to the nonlinear regime, the Airy³ light bullets maintain their robustness, resisting spreading both in space and in time. In particular, we show that as the peak power is increased above the critical power for self-focusing P_{cr}, optical filaments, formed inside the major intensity lobes of the Airy, significantly distort the spatial and temporal characteristics of the Airy wave packet. Despite this, as it propagates the Airy³ light bullet gradually recovers in both space and time with only minor energy dissipation at the expense of energy contained in the peripheral low intensity lobes.

Because of the possibility of space-time decoupling, the spatiotemporal intensity of an Airy³ wave packet whose electric field satisfies the linear paraxial wave equation can be written as

$$I(x, y, z) = I_0 \text{Ai}^2\left(\pm \frac{x}{x_0}\right)\text{Ai}^2\left(\pm \frac{y}{y_0}\right)\text{Ai}^2\left(\pm \frac{\tau}{\tau_0} - \frac{(k_0'')^2 z^2}{4\tau_0^4}\right),$$
(1)

where Ai is the Airy function, *x*, *y*, and *z* are the two transverse and the propagation coordinates, respectively, $\tau = t - (z/v_g)$ is the reduced time, v_g is the group velocity

of the wave packet envelope, x_0, y_0, and τ_0 are the two spatial and temporal widths of the wave packet, respectively, and $k_0'' = \partial^2 k / \partial \omega^2$ is the dispersion coefficient of the medium at the central frequency.

The generation of optical Airy beams relies on the fact that the exponentially truncated Airy function is the Fourier transform of a Gaussian distribution with a cubic phase modulation. Therefore, spatial Airy beams can be generated by imposing a cubic phase on a broad Gaussian beam and then using a converging lens to perform a spatial Fourier transformation [8]. Likewise, the temporal Airy is generated by imposing a cubic phase delay on the spectral components of a Gaussian pulse [7,12].

To obtain an Airy temporal profile, we imposed a cubic spectral phase on our initial 35 fs Gaussian laser pulses by using a grating-telescope compressor, similar to the one used by Chong *et al.* [12]. By using this arrangement (for more details, see [18]), Airy pulses with a main lobe pulse duration of ~200 fs (intensity FWHM) were generated. To measure the temporal intensity of the generated Airy pulses, we cross correlated them with a 35 fs Gaussian reference pulse using a noncollinear second-order cross-correlation technique. It is important to mention that for the short reference pulse duration, this cross correlation (XC) signal matches very closely the intensity distribution of the pulse being measured.

On the other hand, imposing a spatial cubic phase on an intense Gaussian beam is not a trivial task. The low optical damage threshold of spatial light modulators [7,8,19] and the lack of tunability of phase masks [9] are restrictive for the applications in the case of ultraintense Airy beams. Recently, we have demonstrated [19] a simple and convenient method using conventional optical elements that takes advantage of coma aberration to impose a continuous cubic phase and create tunable one- and two-dimensional Airy beams with the capability of handling high intensities. Following this approach [18], we spatially transformed our Gaussian beam into a 2D Airy with a main lobe size of ~200 μm. For our experimental arrangement, the primary Airy[3] lobe contained ~3% of the total spatiotemporal energy content of the wave packet.

In order to confirm the nonspreading behavior of the generated Airy[3] linear wave packets, we studied their propagation through the bulk of transparent polymer samples [PMMA: poly(methyl methacrylate)]. According to third-order susceptibility measurements [20], the critical power for self-focusing in PMMA is estimated to be $P_{cr} \approx$ 1.85 MW (corresponds to 0.36 μJ at 200 fs). Taking this into account, the total pulse energy for linear propagation was set at 200 nJ, corresponding to ~$P_{cr}/60$ in the primary Airy[3] lobe. To characterize the extended propagation of such wave packets, we compared their propagation to a Gaussian wave packet having the same dimensions both in space and in time as the primary Airy[3] intensity lobe. The characteristic linear diffraction and dispersion lengths are

then defined as $L_R = \pi n d_0^2 / (2 \ln 2 \lambda_0)$ and $L_D = \tau_0^2 / (4 \ln 2 \text{GVD})$, respectively, where λ_0 is the central wavelength, n is the refractive index, GVD is the group velocity dispersion, and d_0 and τ_0 are the intensity FWHM of the primary Airy[3] lobe in space and time, respectively. In our case, $d_0 = 200$ μm and $\tau_0 = 200$ fs; thus, the diffraction and dispersion lengths inside the PMMA sample are 16.8 and 26 cm, respectively. In the experiments we used 20-, 60-, 100-, and 140-cm-long PMMA samples corresponding to $(1.2L_R, 0.8L_D)$, $(3.6L_R, 2.3L_D)$, $(6L_R, 3.9L_D)$, and $(8.3L_R, 5.4L_D)$. The Airy[3] wave packets were spatially and temporally characterized after exiting the PMMA samples. Figure 1 shows the normalized XC traces of the Airy primary peak and the respective normalized spatial profiles (recorded by using a 12-bit linear CCD camera) after different propagation lengths in PMMA. The 3D intensity isosurface of the experimentally realized Airy[3] bullet is shown in Fig. 2(a). This was obtained by combining the experimentally measured temporal XC trace of Fig. 1(e) with the corresponding spatial intensity distribution. Furthermore, Fig. 2(b) clearly shows that the spatiotemporal dimensions of the Airy[3] wave packet main lobe remain practically invariant within the measured propagation distance. The variation is about 5% (comparable to our error bar), while, for comparison, a Gaussian pulse with the same spatiotemporal extent as the main Airy lobe would have broadened by a factor of 8.4 in space and 5.5 in time over the same propagation distance (140 cm in PMMA). Nonetheless, it is worth noticing that the slight distortion of the spatial profile in Fig. 1(e) is mainly due to the finite truncation of the experimentally realized Airy beam that is known to set a limit on the range of ideal diffractionless propagation [7]. We would like also to comment on the appearance of a small background between the secondary lobes of the Airy[3] wave packet, in both space and time, at early propagation stages. This is the result of a very small residual second-order phase introduced by our experimental apparatus used to produce the Airy[3] wave packet, which though diffracts or disperses quickly, resulting in much cleaner profiles at the latter propagation stages.

Contrary to the linear propagation regime, in the nonlinear regime space-time coupling is unavoidable [2].
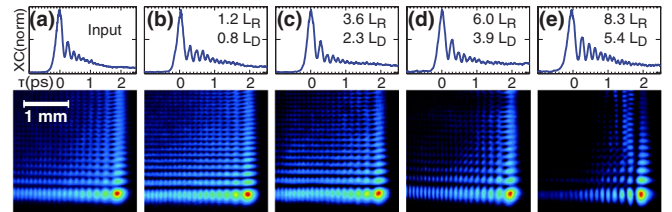

FIG. 1 (color online).   Normalized spatial and temporal profiles of the Airy[3] wave packet: (a) initial and (b)–(e) after propagation through $(1.2L_R, 0.8L_D)$, $(3.6L_R, 2.3L_D)$, $(6L_R, 3.9L_D)$, and $(8.3L_R, 5.4L_D)$, respectively. L_R and L_D are the diffraction and dispersion lengths, respectively.
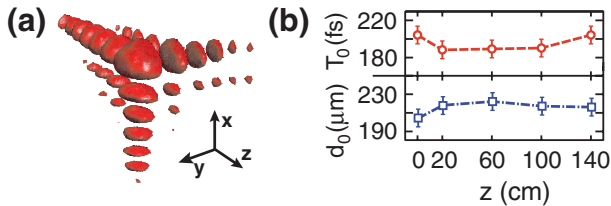
(a)

(b)

FIG. 2 (color online).   (a) Intensity isosurface of the experimentally realized Airy^3 light bullet (to assist visualization, the z axis, time, is stretched by 5 times). (b) Temporal and spatial widths of the Airy^3 wave packet's main lobe vs propagation distance.

Therefore, important questions arise: How intense can an Airy^3 light bullet be before the nonlinear propagation effects take over? Would the bullet be destroyed by such effects, or would it recover?

To answer these questions, we experimentally studied the nonlinear propagation of Airy^3 light bullets in PMMA by monitoring the spatiotemporal profile after propagation through a 2.5-cm-long PMMA sample for different pulse energies. One could expect that as the energy is increased, the primary Airy^3 peak, as well as some of the side lobes containing peak powers above P_{cr}, would be affected by strong nonlinear propagation effects like filamentation. The typical length of a light filament in condensed media ranges from tens of microns to several millimeters while the typical diameter is of the order of 10 μm [14,21]. Figures 3(a)–3(c) show the spatial profiles of the Airy^3 bullet at the exit surface as a function of the total input energy. By comparing to the linear regime, it is clear that as the energy is increased to 0.4 mJ, the spatial Airy profile is distorted and an intense hot spot appears in the main lobe. The transverse dimensions of this hot spot agree well with the typical filament diameter in solid media. As the input energy is further increased [Figs. 3(b) and 3(c)], similar hot spots emerge in the adjacent secondary lobes in both transverse directions. Furthermore, multiple hot spots appear in the main Airy peak leading to deterioration of its spatial profile. This behavior is a typical indication of multiple filamentation as the input power exceeds P_{cr} by a considerable amount. This is further supported by the
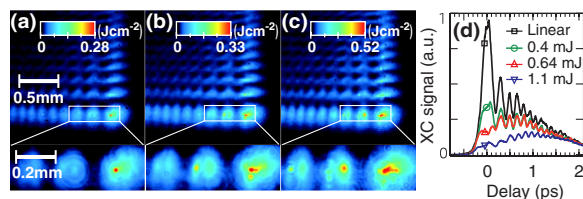

FIG. 3 (color online).   Spatial profiles, representing the fluence distribution, of the Airy^3 light bullet at the exit surface of a 2.5-cm-long PMMA sample for (a) 0.4, (b) 0.64, and (c) 1.1 mJ total energies. (d) Respective temporal profiles at a distance of 20 cm from the sample exit.

strong changes observed in the temporal domain. The corresponding XC traces of the main spatial lobe are shown in Fig. 3(d) as a function of the input energy. It is clear that with an increase of the input energy the effect of nonlinear propagation becomes progressively more profound, resulting in a severe distortion of the Airy temporal profile. Because of the limitations imposed by the finite size of the XC setup, temporal profiles were measured at a distance of 20 cm from the exit face of the sample. Our results show that above a certain input energy (0.4 mJ in our case) strong nonlinear spatiotemporal effects take place during the propagation of intense Airy^3 light bullets. Below this threshold, in a regime which we refer to as weakly nonlinear, the Airy^3 propagates practically in a linear fashion.

Although the Airy^3 light bullets are distorted by the presence of nonlinear effects, one has to bear in mind that these effects are intensity-dependent and predominantly take place in the primary intensity lobes. For an Airy beam, which is not heavily truncated, the amount of energy contained in these lobes can be a relatively small fraction of the total energy (3% in our case). In this perspective, the nonlinear propagation effects such as multiphoton absorption, ionization, and filamentation which lead to the deterioration of the primary intensity lobes both in space and in time can be envisioned as dynamic obstacles to the intense Airy^3 light bullet. Thus, since most of the energy is contained in the secondary lobes which propagate linearly, one should expect the spatiotemporal bullet profile to gradually recover within some propagation distance. This effect should be even more profound if the nonlinear effects are abruptly switched off so that the pure action of the linear Airy spatiotemporal energy flux would heal the nonlinearly induced changes of the Airy^3 spatiotemporal profile.

In order to check this scenario where the self-healing properties of Airy^3 light bullets play an important role [22], we exploited the fact that optical nonlinearities of PMMA and air differ by several orders of magnitude. Hence, for the Airy^3 light bullet, exiting the PMMA sample (where the propagation is nonlinear) is equivalent to an abrupt switch from a nonlinear to a linear propagation regime. Figure 4(a) depicts the spatial profile of the Airy^3 bullet with total energy of 0.4 mJ at the exit surface of the PMMA sample. As was already discussed, at this energy a single filament is formed in the main lobe of the Airy beam. The spatial profile of the same beam after additional propagation of 9 cm in air is shown in Fig. 4(b). Clearly, 9 cm of linear propagation is enough to reconstruct the characteristic spatial profile of the Airy light bullet. Nevertheless, the XC traces recorded at an even further distance of 20 cm from the PMMA exit, shown by the red curve in Fig. 4(c), still exhibit the severe distortion of the main temporal peak of the Airy^3 light bullet. However, complete temporal self-healing occurs after 80 cm of propagation in air as shown
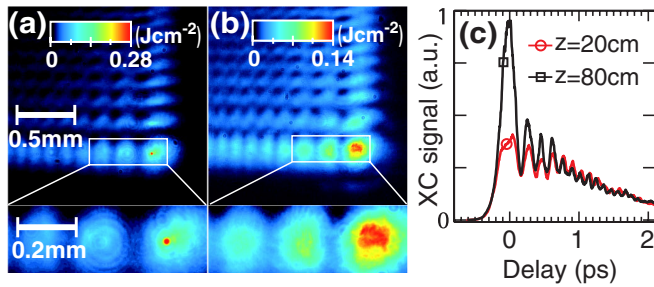
FIG. 4 (color online).   Spatial profiles, representing the fluence distribution, of the Airy³ light bullet with total energy of 0.4 mJ (a) at the exit surface of the sample and (b) after $z = 9$ cm of propagation in air. (c) Respective temporal profiles at $z = 20$ cm ($\bigcirc$) and $z = 80$ cm ($\square$) after the exit surface of the sample.

by the black curve in Fig. 4(c). It is worth mentioning here that, since the energy flux rate towards the main lobe of the bullet is not necessarily symmetric in space and time, the respective healing rates differ as well. Therefore, complete spatial and temporal self-healing occurs after different propagation distances in air. Similar behavior was also observed after propagation in long PMMA samples where the Airy³ spatiotemporal profile fully recovered at the exit surface of the sample.

In summary, we have demonstrated the formation of Airy³ light bullets, which represent a novel type of spatio-temporally nonspreading and robust wave packets capable of simultaneously resisting both dispersion and diffraction. In the high intensity regime, nonlinear effects materialize in the presence of filaments in the primary spatial lobes and distortion of the Airy temporal profile. However, if the nonlinear effects are weak enough, the energy reservoir in the secondary lobes heals the distortions and recon-structs the spatiotemporal profile of the Airy³ light bullet. In addition to nonspreading and robustness properties, temporal and transverse spatial acceleration (bending) of these bullets can be exploited in many applications in different fields such as tomography, microscopy, and long-range signal transmission as well as biological appli-cations. Furthermore, the formation of these bullets paves

the way for the experimental realization of 3D light bullet interactions.

*Corresponding author.
dabdolah@iesl.forth.gr.
†stzortz@iesl.forth.gr; http://unis.iesl.forth.gr.

[1] Y. Silberberg, Opt. Lett. **15,** 1282 (1990).
[2] B. A. Malomed et al., J. Opt. B **7,** R53 (2005).
[3] P. L. Kelley, Phys. Rev. Lett. **15,** 1005 (1965).
[4] J. Durnin, J. J. Miceli, and J. H. Eberly, Phys. Rev. Lett. **58,** 1499 (1987).
[5] P. Di Trapani et al., Phys. Rev. Lett. **91,** 093904 (2003).
[6] M. A. Porras and P. Di Trapani, Phys. Rev. E **69,** 066606 (2004).
[7] G. A. Siviloglou and D. N. Christodoulides, Opt. Lett. **32,** 979 (2007).
[8] G. A. Siviloglou et al., Phys. Rev. Lett. **99,** 213901 (2007).
[9] P. Polynkin et al., Science **324,** 229 (2009).
[10] T. J. Eichelkraut et al., Opt. Lett. **35,** 3655 (2010).
[11] M. V. Berry and N. L. Balazs, Am. J. Phys. **47,** 264 (1979).
[12] A. Chong et al., Nat. Photon. **4,** 103 (2010).
[13] J. C. Gutiérrez-Vega, M. D. Iturbe-Castillo, and S. Chávez-Cerda, Opt. Lett. **25,** 1493 (2000).
[14] A. Couairon and A. Mysyrowicz, Phys. Rep. **441,** 47 (2007).
[15] S. Tzortzakis et al., Phys. Rev. E **64,** 057401 (2001).
[16] S. Tzortzakis, D. Anglos, and D. Gray, Opt. Lett. **31,** 1139 (2006).
[17] J. Kasparian et al., Science **301,** 61 (2003).
[18] See supplementary material at http://link.aps.org/supplemental/10.1103/PhysRevLett.105.253901 for more details on the experimental procedure.
[19] D. G. Papazoglou et al., Phys. Rev. A **81,** 061807 (2010).
[20] F. D'Amore et al., Opt. Mater. (Amsterdam) **24,** 661 (2004).
[21] S. Tzortzakis et al., Phys. Rev. Lett. **87,** 213902 (2001).
[22] J. Broky et al., Opt. Express **16,** 12 880 (2008).